Discovery of N-hydroxy-4-(1H-indol-3-yl)butanamide as a histone deacetylase inhibitor

Jiang Bian, Yepeng luan, Chunbo Wang*, Lei Zhang*

School of Pharmacy, Qingdao University, Qingdao, Shandong, China.

| Summary | The indoles plant growth hormones have exhibited potentially antitumor activities. However, the targets of these indoles have not been clearly elucidated. By introduction of hydroxamic acid group to the structure of indolebutyric acid, the derived molecule (IBHA) exhibited potent HDAC2 (IC_{50} value of 0.32 ± 0.02 μM) and HDAC3 (IC_{50} value of 0.14 ± 0.01 μM) inhibitory activities compared with SAHA (IC_{50} value of 1.25 ± 0.06 μM and 0.97 ± 0.04 μM against HDAC2 and HDAC3). In the antiproliferative assays, the tested hematologic cell lines (U937 and K562) are more sensitive to IBHA than the solid tumor cell lines (MDA-MB-231 and PC-3). In the docking studies, the derived molecule (IBHA) could bind to the active site of human HDAC2 and HDAC3 by strong H-bond interactions and hydrophobic interactions. Pharmacophore mapping results revealed that properties of IBHA matches the receptor (HDAC3) based pharmacophore model. |

Keywords: HDACs inhibitor, indolebutyric acid, hydroxamic acid, docking, pharmacophore model

1. Introduction

Histone deacetylases (HDACs) are a family of enzymes responsible for the deacetylation of histone proteins by removing the acetyl moiety from the amino group of lysine residues on the N-terminal extension of core histones (*1-3*). Eighteen different HDAC isoforms which are divided into four classes have been identified in human. HDAC1, 2, 3 and 8 are classified as class I HDACs; class II HDACs are further subdivided into class IIa (HDAC4, 5, 7, and 9) and IIb (HDAC6 and 10); class III HDACs are a group of NAD+ dependent proteases known as sirtuins (sirt 1-7); Class IV HDACs (HDAC11), is an atypical category of its own.

Overexpression and aberrant recruitment of HDACs (especially class I and II HDACs) have significant roles in the genesis and development of tumor (*4*). Inhibition of HDACs has exhibited potent antitumor potential by induction of biological effects including apoptosis, cell cycle arrest, necrosis, autophagy, differentiation and migration (*5,6*). A number of structurally diverse HDAC inhibitors (HDACIs) have shown potent antitumor efficacy in various stage of clinical trials. Three HDACIs SAHA (*7*), FK228 (*8*) and PXD101 (*9*) have been approved by the US Food and Drug Administration (FDA) for the treatment of cancers.

The indoles plant growth hormones such as naphthaleneacetic acid, indolebutyric acid, indoleacetic acid and the widely studied indole-3-carbinol have showed antitumor potential in human (*10*). However, the targets of these molecules have not been detailed elucidated. Interestingly, the structure of indolebutyric acid is coincide with the pharmacophore of the classic histone deacetylase inhibitors (HDACIs) (Figure 1). The indol ring represents the cap of the HDACIs; the $(CH_2)_3$ of the butyric acid part is the linker; and the carboxylic acid group is the zinc binding group (ZBG). Therefore, hydroxamic acid group was introduced to indolebutyric acid, and the target compound (IBHA) was synthesized and evaluated by the enzymatic inhibition assay. The binding pattern of the designed molecule (IBHA) was predicted by the docking process. Pharmacophore modeling was also performed to evaluate the inhibitor-receptor binding.
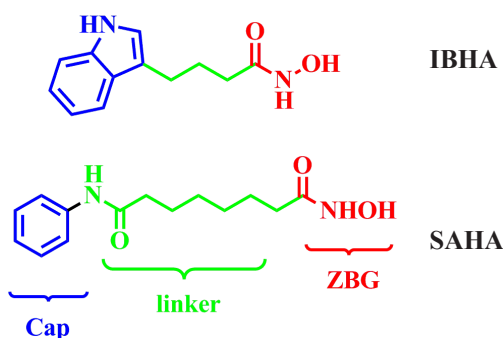
Figure 1. Structural comparison of IBHA with SAHA.

2. Materials and Methods

2.1. *Chemistry*

Target compound IBHA was derived by a single step reaction. The hydroxamic acid group was introduced by coupling of indolebutyric acid (Aladdin, Shanghai, China) and NH_2OH (Aladdin, Shanghai, China) using isobutyl chloroformate (Aladdin, Shanghai, China).

1H NMR spectra were recorded on a Bruker DRX spectrometer at 400 MHz, δ in parts per million and J in hertz, using TMS as an internal standard. High-resolution mass spectra were conducted by Shandong Analysis and Test Center in Ji'nan, China. ESI-MS were determined on an API 4000 spectrometer. Melting points were determined uncorrected on an electrothermal melting point apparatus.

N-hydroxy-4-(1H-indol-3-yl)butanamide (IBHA) To a solution of IBA (1.02 g, 5 mmol) in THF (50 mL), Et_3N (0.51g, 5 mmol) and IBCF (0.75 g, 5.5 mmol) were added in turn. After 10 min, NH_2OH (0.33 g, 10 mmol) was added. The reaction solution was stirred at room temperature for 8 h. Then, the solvent was evaporated with the residue being taken up in saturated citric acid (50 mL) and extracted with EtOAc (3 × 20 mL). The EtOAc solution was washed with brine (3 × 20 mL), dried over $MgSO_4$, and evaporated under vacuum. The desired compound IBHA (0.53 g, 49% yield) was derived by crystallization in EtOAc as white powder. Mp: 198-200 oC. ^{1}H NMR (400 MHz, $(CD_3)_2SO$) δ 11.59 (s, 1H), 10.79 (s, 1H), 10.77 (s, 1H), 7.53-7.50 (m, 1H), 7.33 (d, *J* = 8.0 Hz, 1H), 7.13 (d, *J* = 5.6 Hz, 1H), 7.07-7.04 (m, 1H), 6.96 (t, *J* = 7.2 Hz, 1H), 2.77-2.69 (m, 2H), 2.18 (t, *J* = 7.2 Hz, 2H), 1.95-1.88 (m, 2H). ESI-MS: m/z: 219.3 $[M+H]^+$.

2.2. *Enzyme inhibition assay*

The method of enzymatic inhibition assay has been described in our previous work (*11*). Boc-Lys (acetyl)-AMC was used as the substrate of HDAC; and SAHA was used as a positive control. IBHA was diluted to six concentrations (25, 5, 1, 0.2, 0.04 and 0.008 uM/L) to investigate its HDAC inhibitory ability.

2.3. *In vitro antiproliferative assay*

Tumor cell inhibition was determined by the MTT method. Briefly, 2,000 cells were seeded into each well of 96-well plates, which were incubated at 37°C, 5% CO^2 overnight. The cells were then treated with compound sample at various concentrations for 48 h. After that, a 0.5% MTT solution was added to each well. After 4 h incubation, formazan was extracted by adding DMSO (200 mL) for 5 min. Optical density values were then detected at λ = 570 nm on a micro-plate reader.

2.4. *Molecular docking*

The molecular docking process was performed using Glide software (schrodinger Inc., supported by Shanghai Institute of Materia Medica Chinese Academy of Sciences). Crystal structure of HDAC2 (PDB Entry: 4LXZ), and HDAC3 (PDB Entry: 4A69) were obtained from the RCSB PDB data bank (*www.pdb.org*). Structural optimizations were performed to make the protein suitable for docking. The water molecules and the ligand crystallized in the protein structures were removed, and OPLS 2005 force field was assigned. The ligands used in the docking approach were sketched by maestro and refined by LigPrep. The active site was defined as a cubic box containing residues around Zn ion at a distance of 20 Å. Extra precision was applied in the docking process; other parameters were set as default.

2.5. *Pharmacophore modeling*

Discovery studio 2.5 software was used in the pharmacophore modeling process. The structure of IBHA-HDAC3 used in the present research was derived from the docking study. Structure of HDAC3 was defined as the receptor, and the binding site was defined as a sphere centered on IBHA with radius of 9 Å. Density of lipophilic sites and density of polar sites were set to be 25. The generated features were clustered and only the IBHA surrounding features were kept.

3. Results and Discussion

In order to evaluate the enzymatic inhibition activity and validate the assumption, the activity assay was performed. In this process, IBHA was tested against human HDAC2 and HDAC3 using SAHA as a positive control. The results showed that IBHA is a potent HDAC inhibitor with IC_{50} values of 0.32 ± 0.02 μM and 0.14 ± 0.01 μM against HDAC2 and HDAC3, respectively. Moreover, in the present test, molecule IBHA exhibited better performance than SAHA which showed IC_{50} value of 1.25 ± 0.06 μM and 0.97 ± 0.04 μM against HDAC2 and HDAC3, respectively.

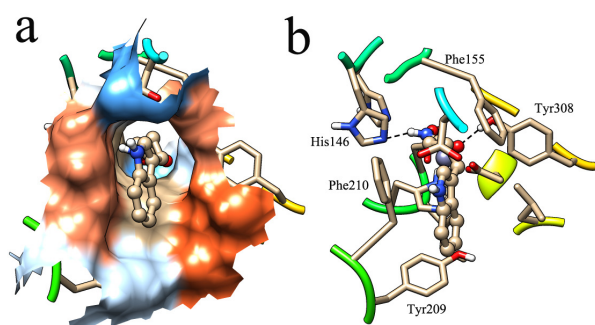To investigate the antiproliferative activity of IBHA,

Figure 2. Results of binding IBHA to the active site of HDAC2. a: surface representation of the ligand-receptor binding; **b**: 3D representation of the interactions.
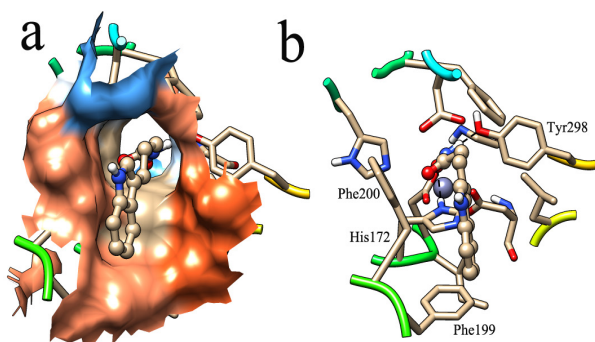

Figure 3. Results of binding IBHA to the active site of HDAC3. a: surface representation of the binding in the active site; **b**: 3D representation of the binding.

MTT assays were performed against 4 types of tumor cell lines. According to the results, IBHA exhibited inhibitory selectivity of hematologic cell lines (U937 and K562) compared with the tested solid tumor cell lines (MDA-MB-231 and PC-3). IBHA displayed IC_{50} values of 9.35 ± 0.12 μM and 11.76 ± 0.55 μM against U937 and K562 cell lines compared with SAHA (1.67 and 1.86 μM), respectively. While the IC_{50} values of IBHA against MDA-MB-231, PC-3 cell lines were 29.87 ± 1.44, 37.6 ± 2.18 μM compared with SAHA (2.91, 4.63 μM), respectively.

In order to predict the binding mode of IBHA in the active sites of HDAC2 and HDAC3, molecular docking approaches were performed using the Glide software. The docking results reveal that IBHA can access to the active site of both HDAC2 and HDAC3 (Figures 2 and 3). The surface plot revealed that the structure of IBHA has good spatial match in the sites, and hydrophobic interactions make significant contributions to the ligand-receptor bindings (Figure 2a and 3a). In the active site of HDAC2, there is significant π-π stacking interaction between the indole group of IBHA and phenyl ring of Phe210 (Figure 2b). Phe199 and Phe200 of HDAC3 play important roles in the hydrophobic interactions by Pi interactions (Figure 3b).

The hydroxamic acid group of IBHA not only chelates to the zinc ions in the active sites as expected, but also generates multiple H-bond interaction with
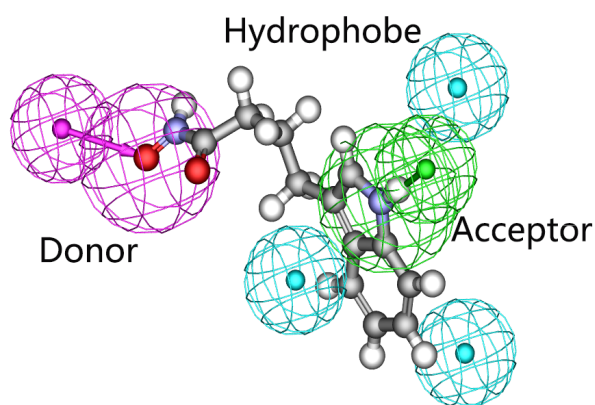

Figure 4. IBHA in the pharmacophore model of HDAC3.

surrounding residues. In the active site of HDAC2, CO of the hydroxamic acid group can form H-bond interactions with OH of Tyr308, and NH has H-bond interactions with NE2 of His146 (Figure 2b). In the catalytic site of HDAC3, the hydroxamic acid group of IBHA binds to His172 and Tyr298 with H-bond interactions (Figure 3b). All these involved interactions make IBHA bind tightly to the active sites of both HDAC2 and HDAC3.

Pharmacophore modeling was performed to further study the ligand-receptor interactions, and a receptor based pharmacophore model was generated on the active site of HDAC3 (Figure 4). The indole ring of IBHA located in the region that is rich in hydrophobic sites, and strong hydrophobic interaction can be formed. The superposition of the NH in the indole ring of IBHA and the H-bond receptor of the pharmacophore model reveals significant H-bond interactions. The NO of the hydroxamic acid group in the region of H-bond donor also make contributions to the H-bond interactions. The pharmacophore modeling results are consistent with that of the docking analysis.

In conclusion, structural modification was performed to make the indoles with antitumor potential (indolebutyric acid) bind to HDACs. Enzymatic inhibition assay results revealed that IBHA could potently inhibit the activity of both HDAC2 and HDAC3. Molecular docking studies showed that the designed molecule (IBHA) can bind to the active site of HDAC2 and HDAC3. Multiple H-bond interactions, hydrophobic interactions such as π-π conjugation and strong chelation, make significant contributions to the IBHA-HDACs bindings. The pharmacophore modeling results displayed good match between the structure of IBHA and the receptor based pharmacophore model. The present work revealed that IBHA could be used a lead compound in the development of novel HDACIs.

Acknowledgements

References

1. Bernstein BE, Tong JK, Schreiber SL. Genomewide studies of histone deacetylase function in yeast. Proc Natl Acad Sci U S A. 2000; 97:13708-13713.
2. De Ruijter AJM, Van Gennip AH, Caron HN, Kemp S, Van Kuilenburg ABP. Histone deacetylases (HDACs): characterization of the classical HDAC family. Biochem J. 2003; 370:737-749.
3. Foglietti C, Filocamo G, Cundari E, De Rinaldis E, Lahm A, Cortese R, Steinkuhler C. Dissecting the biological functions of *Drosophila* histone deacetylases by RNA interference and transcriptional profiling. J Biol Chem. 2006; 281:17968-17976.
4. Marks PA, Rifkind RA, Richon VM, Breslow R, Miller T, Kelly WK. Histone deacetylases and cancer: causes and therapies. Nat Rev Cancer. 2001; 1:194-202.
5. Thiagalingam S, Cheng KH, Lee HJ, Mineva N, Thiagalingam A, Ponte JF. Histone deacetylases: unique players in shaping the epigenetic histone code. Ann N Y Acad Sci. 2003; 983:84-100.
6. Marks PA, Richon VM, Rifkind RA. Histone deacetylase inhibitors: inducers of differentiation or apoptosis of transformed cells. J Natl Cancer Inst. 2000; 92:1210-1216.
7. Richon VM, Emiliani S, Verdin E, Webb Y, Breslow R, Rifkind RA, Marks PA. A class of hybrid polar inducers of transformed cell differentiation inhibits histone deacetylases. Proc Natl Acad Sci U S A. 1998; 95:3003-3007.
8. Ueda H, Nakajima H, Hori Y, Fujita T, Nishimura M, Goto T, Okuhara M. FR901228, a novel antitumor bicyclic depsipeptide produced by *Chromobacterium violaceum* No. 968. I. Taxonomy, fermentation, isolation, physico-chemical and biological properties, and antitumor activity. J Antibiot (Tokyo). 1994; 47:301-310.
9. Yang L, Xue XW, Zhang YH. Simple and Efficient Synthesis of Belinostat. Synthetic Commun. 2010; 40:2520-2524.
10. Kline BE, Rusch HP. Tumor inhibitor studies II. The effect of plant hormones on tumor growth. Cancer Res. 1943; 3:702-705.
11. Zhang YJ, Feng JH, Liu CX, Zhang L, Jiao J, Fang H, Su L, Zhang XP, Zhang J, Li MY, Wang BH, Xu WF. Design, synthesis and preliminary activity assay of 1,2,3,4-tetrahydroisoquinoline-3-carboxylic acid derivatives as novel Histone deacetylases (HDACs) inhibitors. Bioorgan Med Chem. 2010; 18:1761-1772.